



The following Communications have been judged by at least two referees to be “very important papers” and will be published online at www.angewandte.org soon:

R. M. Culik, A. L. Serrano, M. R. Bunagan,* F. Gai*
Achieving Secondary Structural Resolution in Kinetic Measurements of Protein Folding: A Case Study of the Folding Mechanism of Trp-cage

X. Xin, M. He, W. Han, J. Jung, Z. Lin*
Low-Cost Counter Electrodes for High-Efficiency Dye-Sensitized Solar Cells

Y. Filinchuk,* Bo Richter, T. R. Jensen,* V. Dmitriev, D. Chernyshov, H. Hagemann

Porous and Dense $Mg(BH_4)_2$ Frameworks: Synthesis, Stability, and Reversible Absorption of Guest Species

A. Ardèvol, C. Rovira*
The Molecular Mechanism of Enzymatic Glycosyl Transfer with Retention of Configuration: Evidence for a Short-Lived Oxocarbenium Ion Like Species

C. Zhang, Z. Xu, L. Zhang, N. Jiao*
Copper-Catalyzed Aerobic Oxidative Coupling of Aryl Acetaldehydes with Anilines Leading to α -Ketoamides

M. E. Weiss, E. M. Carreira*
Total Synthesis of (+)-Daphmanidin E

J. Bacsá, F. Hanke, S. Hindley, R. Odra, G. R. Darling, A. C. Jones, A. Steiner*

The Solid-State Structures of Dimethylzinc and Diethylzinc

K. E. Shopsowitz, W. Y. Hamad, M. J. MacLachlan*
Chiral Nematic Mesoporous Carbon Derived from Nanocrystalline Cellulose

Z.-C. Wang, N. Dietl, R. Kretschmer, T. Weiske, M. Schlangen,* H. Schwarz*

Catalytic Redox Reactions in the CO/N_2O System Mediated by the Bimetallic Oxide-Cluster Couple $AlVO_3^+/AlVO_4^+$

C. D. N. Gomes, O. Jacquet, C. Villiers, P. Thuéry, M. Ephritikhine, T. Cantat*

A Diagonal Approach to Chemical Recycling of Carbon Dioxide: New Organocatalytic Transformation for the Reductive Functionalization of CO_2



„In a spare hour I would like to run at sunset or sunrise. The biggest challenge facing scientists is to keep their autonomy and independence and preserve spare time for creativity. ...“
 This and more about Andreas Kirschning can be found on page 10488.

Author Profile

Andreas Kirschning _____ 10488



D. Shechtman

News

Nobel Prizes 2011
 Chemistry: D. Shechtman _____ 10489

Ion Mobility Spectrometry –
 Mass Spectrometry

Charles L. Wilkins, Sarah Trimpin

Books

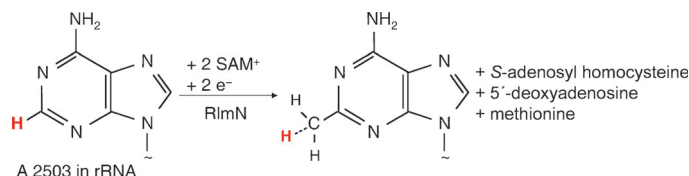
reviewed by D. Schröder _____ 10490

Highlights

Enzymatic C-Methylation

W. Buckel, R. K. Thauer* – 10492 – 10494

Dual Role of S-Adenosylmethionine (SAM⁺) in the Methylation of sp²-Hybridized Electrophilic Carbons



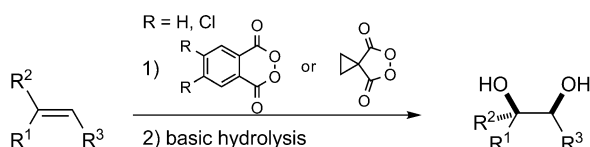
A surprising mechanism: The enzymatic methylation of adenosine at C-2 consumes two molecules of S-adenosylmethionine (SAM⁺), one in the S_N2 transfer of its methyl group to an active-site cysteine of the methyltransferase, and a

second in the formation of a 5'-deoxyadenosine radical (5'-A[•]) that abstracts a hydrogen atom from the protein-bound methyl group enabling it to attack at C-2 of the adenosine (see scheme).

Alkene Dihydroxylation

M. Schwarz, O. Reiser* – 10495 – 10497

Metal or No Metal: That Is the Question!



Dihydroxylation with peroxides: The 1,2-dihydroxy structural motif, which can be generated from a C=C bond, occurs widely in organic compounds. Advances in the *syn* dihydroxylation of alkenes with cyclic

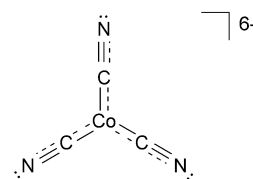
acyl peroxides broaden the application of this transformation for a variety of olefins (see scheme). In recent studies the scope, limitations, and a mechanistic pathway have been delineated.

Small Molecules

W. Kaim* – 10498 – 10500

“Guilty” Verdict—Evidence for the Noninnocence of Cyanide

More than three centuries after its inadvertent preparation in a coordination compound, the noninnocence of cyanide has been established unequivocally by structural and spectroscopic studies of M₃[Co(CN)₃], M = Ba or Sr. The 18-valence-electron ion [Co(CN)₃]⁶⁻ contains a closed-shell Co^{-I} center and three CN^{1.67-} ligands (see scheme).



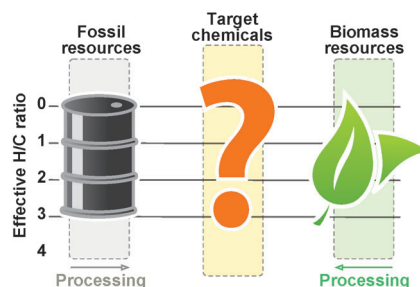
For the USA and Canada: ANGEWANDTE CHEMIE International Edition (ISSN 1433-7851) is published weekly by Wiley-VCH, PO Box 191161, 69451 Weinheim, Germany. Air freight and mailing in the USA by Publications Expediting Inc., 200 Meacham Ave., Elmont, NY 11003. Periodicals

postage paid at Jamaica, NY 11431. US POSTMASTER: send address changes to *Angewandte Chemie*, Journal Customer Services, John Wiley & Sons Inc., 350 Main St., Malden, MA 02148-5020. Annual subscription price for institutions: US\$ 11,738/10,206 (valid for print and electronic / print or electronic delivery); for

individuals who are personal members of a national chemical society prices are available on request. Postage and handling charges included. All prices are subject to local VAT/sales tax.

Essays

From petroleum to bioleum: Since biomass is a limited resource, it is necessary to consider its best use. The production of select chemicals from biomass, rather than its use as fuel, could effectively replace the use of petroleum in the chemical industry, but the inherent functionality of biomass must be exploited (see picture).



Renewable Resources

P. N. R. Vennestrøm, C. M. Osmundsen,
C. H. Christensen,
E. Taarning* _____ 10502–10509

Beyond Petrochemicals: The Renewable
Chemicals Industry

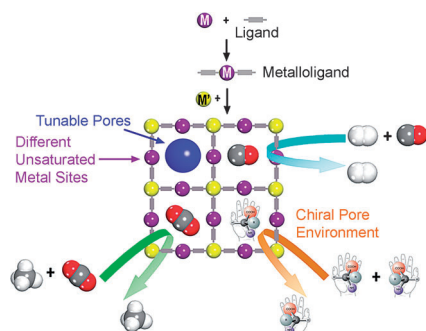


Minireviews

Metal–Organic Frameworks

M. C. Das, S. Xiang, Z. Zhang,
B. Chen* _____ 10510–10520

Functional Mixed Metal–Organic
Frameworks with Metalloligands



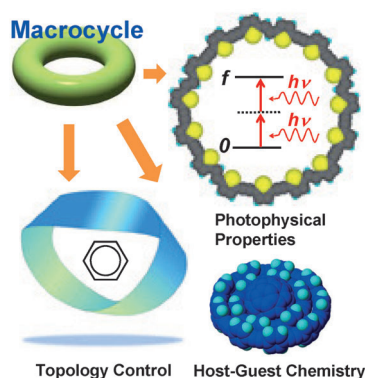
Metal mixer: A novel metalloligand approach allows the rational immobilization of a variety of functional sites in mixed metal–organic frameworks (M'MOFs). This Minireview highlights some important functional M'MOFs with metalloligands for gas storage and separation, enantioselective separation, heterogeneous asymmetric catalysis, sensing, drug delivery, and biomedical imaging.

Reviews

Conjugated Macrocycles

M. Iyoda,* J. Yamakawa,
M. J. Rahman _____ 10522–10553

Conjugated Macrocycles: Concepts and
Applications



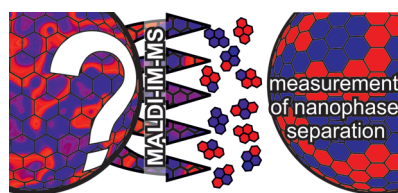
Going in giant circles: Fully unsaturated macrocycles exhibit unusual optical and magnetic behavior because of their effective cyclic conjugation. In particular, site-specific substitution at interior and exterior sites can afford attractive structures for a wide range of research fields such as organic chemistry, polymer and materials science, and supramolecular chemistry.

Communications

VIP Surface Science

K. M. Harkness, A. Balinski,
J. A. McLean,*
D. E. Cliffler* _____ 10554–10559


 Nanoscale Phase Segregation of Mixed Thiolates on Gold Nanoparticles



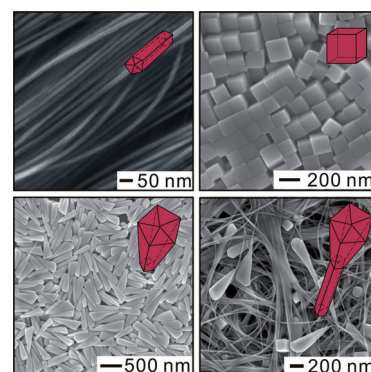
A simple screening method: Phase segregation and domain formation is observed within the protecting monolayer of gold nanoparticles (AuNPs) using ion mobility mass spectrometry (IM-MS), a two-dimensional gas-phase separation technique. Experimental data are compared to a theoretical model. Deviations from this model provide evidence for nanophase separation resulting in anisotropic AuNPs.

Nanoparticle Synthesis

M. Jin, G. He, H. Zhang, J. Zeng, Z. Xie,
Y. Xia* _____ 10560–10564


 Shape-Controlled Synthesis of Copper Nanocrystals in an Aqueous Solution with Glucose as a Reducing Agent and Hexadecylamine as a Capping Agent

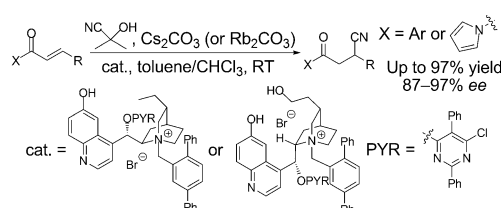
Shape up: Copper nanocrystals with different shapes enclosed mainly by {100} facets have been prepared by reducing CuCl_2 with glucose. The syntheses were performed in an aqueous solution at 100°C with the use of hexadecylamine as a capping agent (see scheme).



Asymmetric Catalysis

B. A. Provencher, K. J. Bartelson, Y. Liu,
B. M. Foxman, L. Deng* _____ 10565–10569

 Structural Study-Guided Development of Versatile Phase-Transfer Catalysts for Asymmetric Conjugate Additions of Cyanide




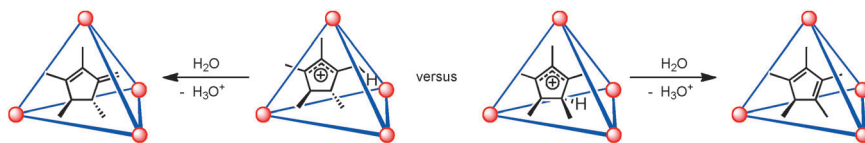
Unprecedented phase-transfer catalysts for the first example of an organocatalytic asymmetric conjugate addition of cyanide with acetone cyanohydrin are reported (see scheme). Utilizing an accessible cupreidinium salt and a cyanation reagent

suitable for industrial scale, this reaction holds significant promise for practical asymmetric synthesis. The catalysts were developed as a result of key structural insights gained by X-ray analysis.

Supramolecular Catalysis

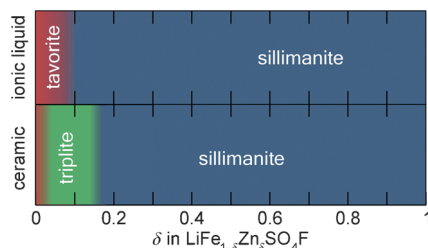
C. J. Hastings, M. P. Backlund,
R. G. Bergman,*
K. N. Raymond* _____ 10570–10573

 Enzyme-like Control of Carbocation Deprotonation Regioselectivity in Supramolecular Catalysis of the Nazarov Cyclization



The kinetically controlled, regioselective deprotonation of cyclopentenyl cations is mediated by encapsulation within a metal–ligand assembly. The regiochemistry of the deprotonation step determines

which one of two possible products is formed. Moreover, subtle differences in the stereochemistry of the encapsulated cation switch the selectivity of this process (see scheme).

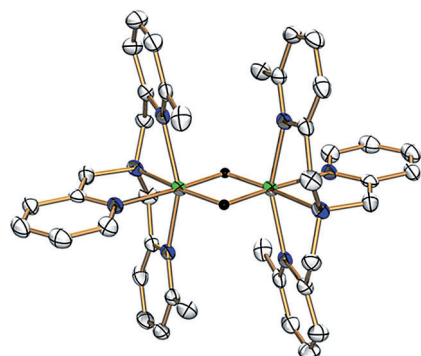


Transition-metal fluorosulfates are currently under intense investigation for their use as anodes in Li-ion batteries. The substitution of Zn into LiFeSO_4F has been found to trigger a transition from the tavorite structure to two separate polymorphs which crystallize in the sillimanite and triplite structures (see picture). These new phases show $\text{Fe}^{2+}/\text{Fe}^{3+}$ redox potentials of 3.6 and 3.9 V versus Li, respectively.

Solid-State Chemistry

M. Ati, B. C. Melot, G. Rousse, J.-N. Chotard, P. Barpanda, J.-M. Tarascon* **10574–10577**

Structural and Electrochemical Diversity in $\text{LiFe}_{1-\delta}\text{Zn}_\delta\text{SO}_4\text{F}$ Solid Solution: A Fe-Based 3.9 V Positive-Electrode Material

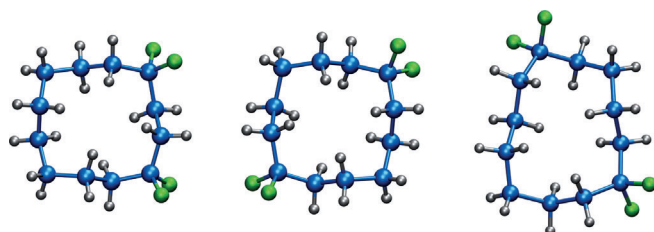


A generous donor: A dinuclear octahedral bis(μ -hydrido)dinickel(II) complex (see picture; C gray, H black, N blue, Ni green) acts as an electron donor to reduce electron acceptors such as methyl viologen. The complex is proposed as a functional model for the dihydride intermediate of an NiRu hydrogenase mimic and, by extension, of [NiFe]hydrogenase itself.

Hydrogenase Mimics

T. Matsumoto, T. Nagahama, J. Cho, T. Hizume, M. Suzuki,* S. Ogo* **10578–10580**

Preparation and Reactivity of a Nickel Dihydride Complex



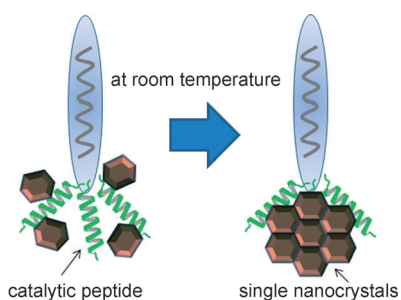
Getting out of the way: In fluorinated cyclododecane structures the CF_2 group locates only at corner positions (see picture). This relaxes 1,4-H,H transannular interactions as a result of C- CF_2 -C angle widening. Misplaced CF_2 groups lead to

significant ring distortion. It follows that strategic incorporation of CF_2 groups has potential as a design feature to introduce order and polarity into organic hydrocarbon structures.

Organofluorine Chemistry

M. Skibinski, Y. Wang, A. M. Z. Slawin, T. Lebl, P. Kirsch, D. O'Hagan* **10581–10584**

Alicyclic Ring Structure: Conformational Influence of the CF_2 Group in Cyclododecanes



Screen saver: A simple and convenient route has been developed that allows peptides that catalyze the growth of the target material to be screened directly. This approach has been used to identify a peptide that induces the catalytic growth of single-crystalline ZnO nanocrystals through a nonclassical crystallization process at room temperature (see picture).

Bioinorganic Chemistry

Z. Wei, Y. Maeda, H. Matsui* **10585–10588**

Discovery of Catalytic Peptides for Inorganic Nanocrystal Synthesis by a Combinatorial Phage Display Approach



Nanocrystal Imaging Agents

T. Kim, E.-J. Cho, Y. Chae, M. Kim, A. Oh,
J. Jin, E.-S. Lee, H. Baik, S. Haam,
J.-S. Suh, Y.-M. Huh,*
K. Lee* 10589–10593



Urchin-Shaped Manganese Oxide Nanoparticles as pH-Responsive Activatable T_1 Contrast Agents for Magnetic Resonance Imaging

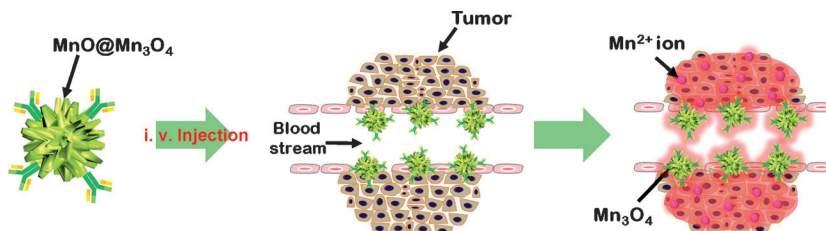


Image enhancement: Core-shell $\text{MnO}@\text{Mn}_3\text{O}_4$ urchin-shaped nanoparticles can be synthesized by means of an anisotropic etching process and used as a pH-activatable T_1 contrast agent for mag-

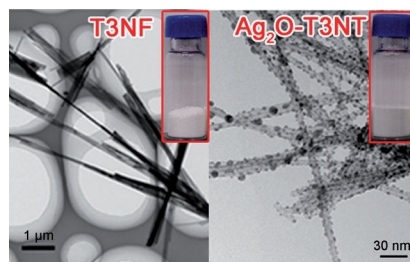
netic resonance imaging. The manganese ions released from the MnO phase in the low-pH sites within tumor cells lead to an enhanced T_1 contrast image for the entire tumor mass.

Nanostructures

D. Yang, S. Sarina, H. Zhu,* H. Liu,
Z. Zheng, M. Xie, S. V. Smith,
S. Komarneni 10594–10598



Capture of Radioactive Cesium and Iodide Ions from Water by Using Titanate Nanofibers and Nanotubes



Going down the tubes: The rapid uptake of $^{137}\text{Cs}^+$ ions in sodium trititanate nanofibers (T3NF; see picture) and nanotubes (T3NT) triggers a phase transition or deformation of the thin titanate layers. Ag_2O nanocrystals (5–10 nm) were bound to the surface of the nanostructures and efficiently captured I^- anions (ca. 4.5 mmol per gram of sorbent) from aqueous solutions by forming an AgI precipitate on the titanates.

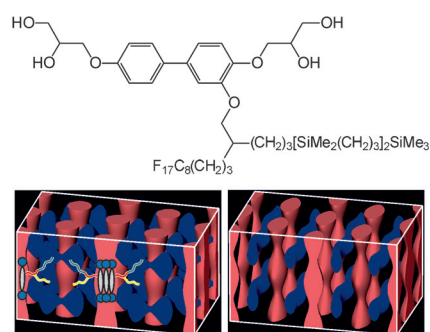
Liquid Crystals

F. Liu, M. Prehm, X. Zeng, G. Ungar,*
C. Tschierske* 10599–10602



Two- and Three-Dimensional Liquid-Crystal Phases from Axial Bundles of Rodlike Polyphiles: Segmented Cylinders, Crossed Columns, and Ribbons between Sheets

Pleated ribbons and bow ties: Rodlike mesogens (see scheme) with swallow-tail side chains arrange axially in ribbonlike bundles. At high temperatures the ribbons rotate, resulting in a novel 3D hexagonal liquid-crystal phase (see picture, left). At lower temperature, rotation locks in giving a structure of crossed aromatic and fluorinated columns (right). On further cooling the ribbons fuse into aromatic sheets with fluorinated columns intercalated.

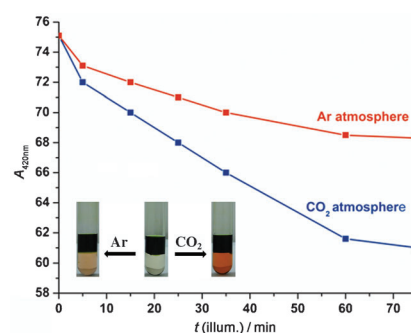


Photosynthesis

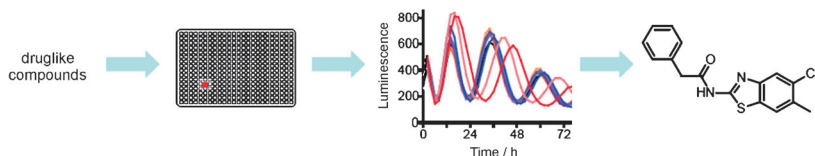
J. Bhuyan, R. Sarkar,
S. Sarkar* 10603–10607



A Magnesium Porphyrin Bicarbonate Complex with CO_2 -Modulated Photosystem I Action



Light to chemical energy: Magnesium tetraphenylporphyrin (MgTPP ; **1**), upon treatment with $[\text{Bu}_4\text{N}]\text{OH}$ under a CO_2 atmosphere, formed its bicarbonate adduct, $[\text{Bu}_4\text{N}][\text{HCO}_3\text{MgTPP}]$ (**2**). Compound **2** is electrochemically oxidized at a lower potential than that of **1**; under light illumination, it drops to an even lower value, resulting in a more facile electron release (see picture).



Time shift: A high-throughput cell-based screen identified a benzothiazole analogue, LH846, which induces period lengthening of the circadian rhythm.

Affinity chromatography coupled with mass spectrometry and genomic analysis identified protein kinase CK1 δ as the biological target of LH846 (see picture).

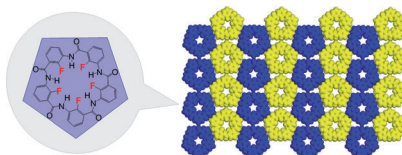
Chemical Biology

J. W. Lee, T. Hirota, E. C. Peters, M. Garcia, R. Gonzalez, C. Y. Cho, X. Wu, P. G. Schultz,* S. A. Kay* **10608–10611**

A Small Molecule Modulates Circadian Rhythms through Phosphorylation of the Period Protein



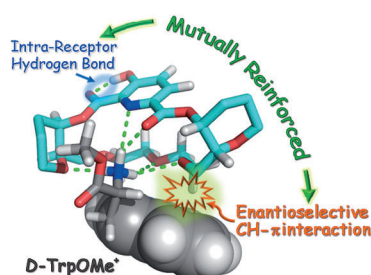
Regular pentagonal adhesive tiles were obtained by designing a cyclic fluoropentamer with an internal CF \cdots HN H-bonded network and “sticky” edges that can glue the molecules together through intermolecular C_AH \cdots O=C H bonds. In the crystal they form the mathematically predicted densest all-pentagon 2D lattice with a packing density of 0.921 (see picture).



2D Pentagon Packing

C. L. Ren, F. Zhou, B. Qin, R. J. Ye, S. Shen, H. B. Su, H. Q. Zeng* **10612–10615**

Crystallographic Realization of the Mathematically Predicted Densest All-Pentagon Packing Lattice by C_s-Symmetric “Sticky” Fluoropentamers



Call in the reinforcements: Intra-receptor noncovalent interactions can enantioselectively cooperate with guest binding, thus triggering chiral discrimination. Such cooperativity is described and quantified for a simple synthetic system wherein an intra-receptor hydrogen bond cooperates with a CH- π interaction exclusively formed with the D enantiomer of the guest, thus exemplifying reinforced chiral recognition (see picture).

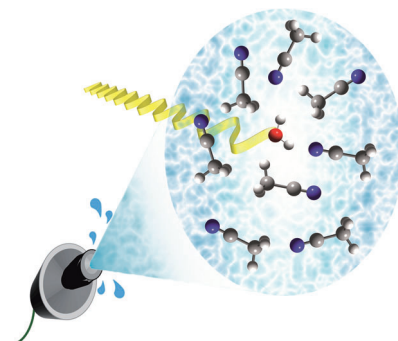
Molecular Recognition

R. Carrillo,* A. Feher-Voelger, T. Martín* **10616–10620**

Enantioselective Cooperativity Between Intra-Receptor Interactions and Guest Binding: Quantification of Reinforced Chiral Recognition



A liquid microjet was used to obtain oxygen K-edge X-ray absorption and emission spectra of water–acetonitrile mixtures of various compositions. The observed spectral changes are unambiguously related to the increasing number of broken hydrogen bonds with decreasing water concentration, and the hydrogen-bond network of liquid water can thus be addressed on purely experimental grounds without the need for theoretical modeling.



Hydrogen Bonds

K. M. Lange, R. Könnecke, M. Soldatov, R. Golnak, J.-E. Rubensson, A. Soldatov, E. F. Aziz* **10621–10625**

On the Origin of the Hydrogen-Bond-Network Nature of Water: X-Ray Absorption and Emission Spectra of Water–Acetonitrile Mixtures





CO₂ Insertion

S. J. Zuend, O. P. Lam, F. W. Heinemann, K. Meyer* — 10626–10630



Carbon Dioxide Insertion into Uranium-Activated Dicarbonyl Complexes

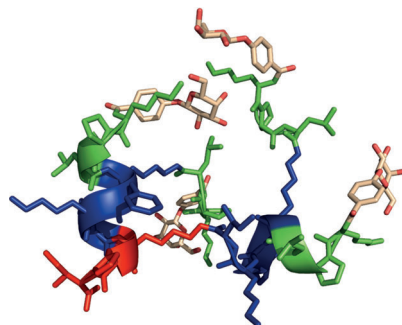
Quick on the uptake: Uranium(III) complexes bearing hexadentate triazacyclononane macrocyclic ligands L¹ engage di- and triketones in both one- and two-electron reduction pathways. The dinu-

clear enolate generated through one of these pathways reacts with carbon dioxide to generate a new C–C bond (see scheme).

Biofilm Inhibitors



R. U. Kadam, M. Bergmann, M. Hurley, D. Garg, M. Cacciarini, M. A. Swiderska, C. Nativi, M. Sattler, A. R. Smyth, P. Williams, M. Cámara, A. Stocker, T. Darbre, J.-L. Reymond* — 10631–10635



Inhibiting factors: Biofilm inhibition is achieved with a phenylgalactosyl peptide dendrimer (see picture) that binds to the galactose-specific lectin LecA of *P. aeruginosa*. The multivalency of the ligands is critical for biofilm inhibition, although the nature of the linker between the peptide dendrimer and the galactose can provide additional contacts to the lectin and also has an effect on the interaction.



A Glycopeptide Dendrimer Inhibitor of the Galactose-Specific Lectin LecA and of *Pseudomonas aeruginosa* Biofilms

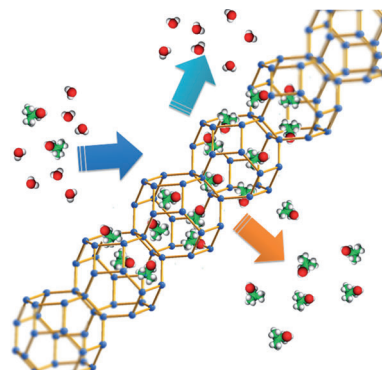
MOF Membranes

X.-L. Liu, Y.-S. Li,* G.-Q. Zhu, Y.-J. Ban, L.-Y. Xu, W.-S. Yang* — 10636–10639



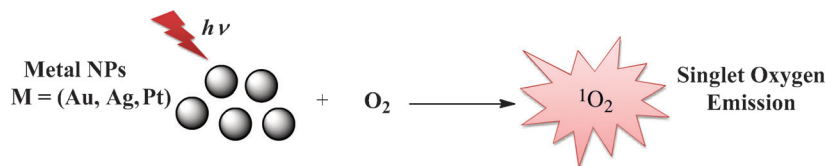
An Organophilic Pervaporation Membrane Derived from Metal–Organic Framework Nanoparticles for Efficient Recovery of Bio-Alcohols

On the road to recovery: The dynamic apertures and superhydrophobic surfaces of the metal–organic framework ZIF-8 result in its extraordinary ability to selectively adsorb alcohols. When incorporated into a polymer matrix, the ZIF-8 nanoparticles provide preferential pathways for the permeation of organic compounds and allow the efficient pervaporative recovery of bio-alcohols from fermentation broths (see picture).



¹O₂ Generation

R. Vankayala, A. Sagadevan, P. Vijayaraghavan, C.-L. Kuo, K. C. Hwang* — 10640–10644

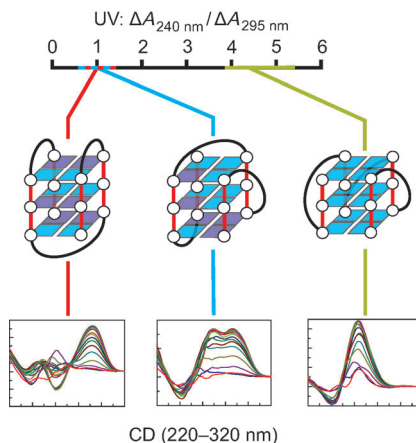


Metal Nanoparticles Sensitize the Formation of Singlet Oxygen

Improving on organic photosensitizers: The photoexcitation of metal nanoparticles results in the formation of singlet oxygen and its phosphorescence emission (see picture). As the nanoparticles are resistant to both photoinduced and enzy-

matic degradation and also have impressively high extinction coefficients, these findings may have an impact on techniques for the generation of singlet oxygen in biological settings.

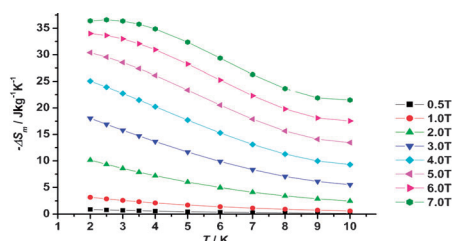
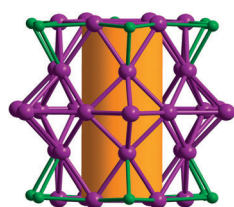
Four-fold: Not just the identification, but also the rapid characterization and classification of nucleic acid G-quadruplexes into topology groups is feasible utilizing UV and circular dichroism (CD) spectroscopy (see picture). It is now possible to utilize inexpensive UV spectroscopy to achieve the same level of characterization previously only possible with CD spectroscopy.



Quadruplex Topologies

A. I. Karsisiotis, N. M. Hessari,
E. Novellino, G. P. Spada,* A. Randazzo,*
M. Webba da Silva* — 10645 – 10648

Topological Characterization of Nucleic Acid G-Quadruplexes by UV Absorption and Circular Dichroism



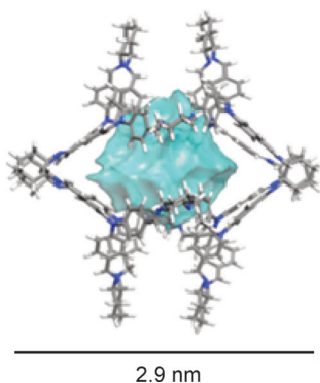
A **tubelike metal cluster** containing 36 Gd and 12 Ni atoms was obtained by anion-templated self-assembly of the metal ions (see picture for arrangement of the 48 metal ions in the cluster core). The huge

cryogenic magnetocaloric effects exhibited by this cluster (see plot of magnetic entropy change ΔS_m) can be rationalized in terms of its large metal/ligand mass ratio.

Magnetocaloric Effect

J.-B. Peng, Q.-C. Zhang, X.-J. Kong,*
Y.-P. Ren, L.-S. Long*
R.-B. Huang, L.-S. Zheng,
Z. Zheng — 10649 – 10652

A 48-Metal Cluster Exhibiting a Large Magnetocaloric Effect



Keep the cage filled: Two large organic cages (see example) with void diameters of 1.2 nm were synthesized through [8+12] imine condensation reactions. The materials become amorphous upon solvent removal and show little permanent porosity. Molecular dynamics simulations give an insight into the mechanism of these processes, suggesting strategies for synthesizing larger shape-persistent organic cages in the future.

Organic cages

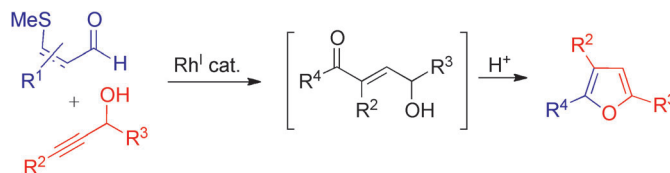
K. E. Jelfs, X. F. Wu, M. Schmidtman,
J. T. A. Jones, J. E. Warren, D. J. Adams,
A. I. Cooper* — 10653 – 10656

Large Self-Assembled Chiral Organic Cages: Synthesis, Structure, and Shape Persistence



Heterocycle Synthesis

P. Lenden, D. A. Entwistle,
M. C. Willis* ————— 10657 – 10660



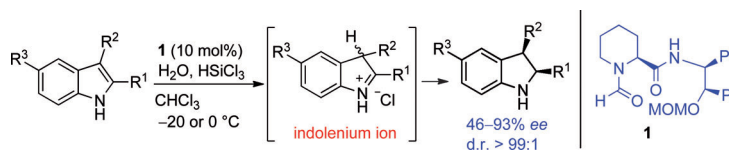
An Alkyne Hydroacylation Route to Highly Substituted Furans

More rings for your rhodium: Rhodium-catalyzed intermolecular alkyne hydroacylations deliver γ -hydroxy- α,β -enones, which can be cyclized in situ to deliver di- and trisubstituted furans. Functionalization of the intermediates using Heck

chemistry allows the formation of regioisomeric furans. The use of an alternative Rh^I catalyst delivers 1,4-dicarbonyl compounds and hence pyrroles, thiophenes, and pyridazines, all from the same two starting materials.

Organocatalysis

Y.-C. Xiao, C. Wang, Y. Yao, J. Sun,*
Y.-C. Chen* ————— 10661 – 10664



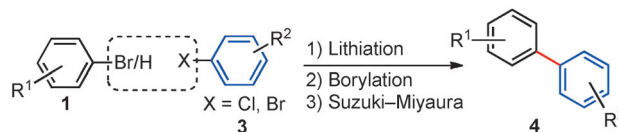
Direct Asymmetric Hydrosilylation of Indoles: Combined Lewis Base and Brønsted Acid Activation

Quite a pair: The first organocatalytic direct asymmetric reduction of unprotected 1H-indoles to chiral indolines has been developed. The reaction proceeds through the generation of electrophilic indolenium ions by a Brønsted acid, and

then chiral Lewis base (**1**) mediated enantioselective hydride transfer with HSiCl₃. A variety of chiral indolines were obtained with moderate to excellent enantioselectivity. MOM = methoxymethyl.

Flow Chemistry

W. Shu, L. Pellegatti, M. A. Oberli,
S. L. Buchwald* ————— 10665 – 10669



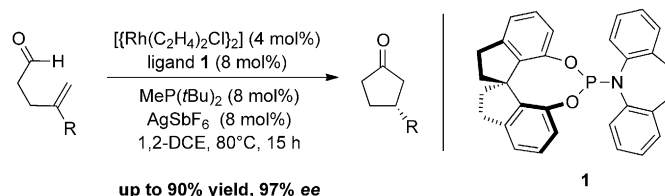
Continuous-Flow Synthesis of Biaryls Enabled by Multistep Solid-Handling in a Lithiation/Borylation/Suzuki–Miyaura Cross-Coupling Sequence

Let it flow: An efficient and modular synthesis of biaryls under continuous-flow conditions has been realized by a lithiation/borylation/Suzuki–Miyaura cross-coupling sequence under ambient conditions. Aryl bromides and heteroaromatic

precursors can be transformed in the room-temperature lithiation reaction with *n*BuLi, followed by borylation and Suzuki–Miyaura coupling with the aid of ultrasonic irradiation (see scheme).

Asymmetric Catalysis

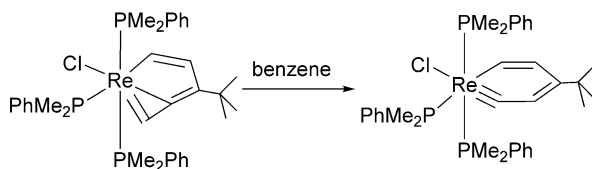
T. J. Hoffman,
E. M. Carreira* ————— 10670 – 10674



Catalytic Asymmetric Intramolecular Hydroacylation with Rhodium/Phosphoramidite–Alkene Ligand Complexes

Give me a P: An asymmetric intramolecular Rh-catalyzed hydroacylation reaction of pent-4-enals for the preparation of functionalized cyclopentanones in good yield and high enantioselectivity is de-

scribed (see scheme, DCE = dichloroethane). This process uses rhodium complexes featuring novel modular phosphoramidite–alkene ligands and achiral phosphine coligands.



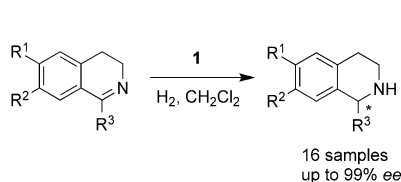
Complex rearrangements: Rhenabenzenes, which are metallaaromatic compounds related to metallabenzenes (see scheme), can be obtained from thermally unstable rhenium–carbyne complexes through rearrangement reactions. The

rhenabenzynes complex was characterized by elemental analysis, ^1H NMR spectroscopy, and X-ray diffraction analysis. The results show that it is possible to prepare metallabenzenes with different transition metals.

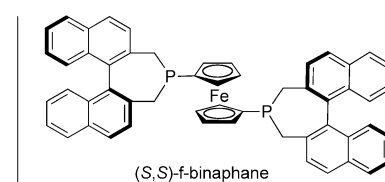
Metallacycles

J. Chen, H. H. Y. Sung, I. D. Williams, Z. Lin,* G. Jia* **10675–10678**

Synthesis and Characterization of a Rhenabenzynes Complex



Efficient and enantioselective: Using the iodine-bridged dimeric iridium complex $[\{\text{Ir}(\text{H})[(S,S)\text{-}(\text{f})\text{-binaphane}]\}_2(\mu\text{-I})_3]^+\text{I}^-$ (**1**) a wide range of tetrahydroisoquinoline alkaloids, including the substructure of



the pharmaceutical drug solifenacin, were obtained with excellent enantioselectivities and high turnover numbers (see scheme).

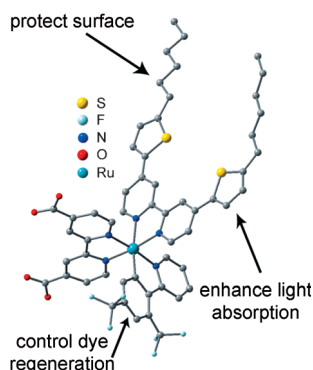
Asymmetric Catalysis

M. Chang, W. Li, X. Zhang* **10679–10681**

A Highly Efficient and Enantioselective Access to Tetrahydroisoquinoline Alkaloids: Asymmetric Hydrogenation with an Iridium Catalyst



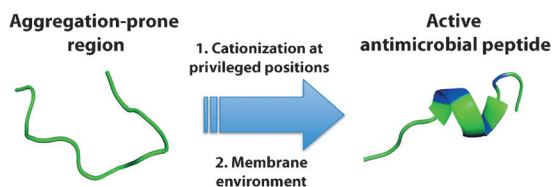
A trisheteroleptic cyclometalated ruthenium complex (see picture) bearing aliphatic substituents was synthesized, characterized, and evaluated in a dye-sensitized solar cell (DSSC). This thiocyanate-free dye, which has favorable structural elements to exhibit long-term stability, generates a high power output in the DSSC with both iodide-based and Co-based redox shuttles.



Solar Cells

P. G. Bomben, T. J. Gordon, E. Schott, C. P. Berlinguette* **10682–10685**

A Trisheteroleptic Cyclometalated Ru^{II} Sensitizer that Enables High Power Output in a Dye-Sensitized Solar Cell



Action stations: Antimicrobial peptides (AMPs) can be derived from amyloid-prone regions by introduction of cationic residues at privileged positions (see picture). The design and testing of 24 de

novo amyloid-derived AMPs are described, and the likelihood of evolution of amyloid-prone protein regions, devoid of antimicrobial activity, into potent antimicrobial domains is addressed.

Antimicrobial Peptides

M. Torrent, J. Valle, M. V. Nogués, E. Boix, D. Andreu* **10686–10689**

The Generation of Antimicrobial Peptide Activity: A Trade-off between Charge and Aggregation?

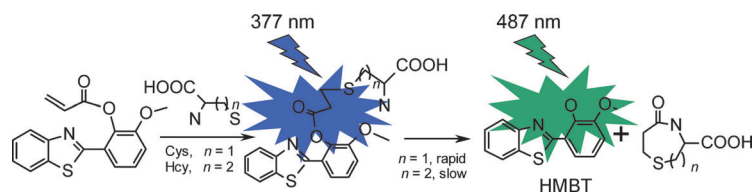


Fluorescent probes

X. F. Yang,* Y. X. Guo,
R. M. Strongin* — 10690 – 10693



Conjugate Addition/Cyclization Sequence Enables Selective and Simultaneous Fluorescence Detection of Cysteine and Homocysteine



Similar but different: A benzothiazole derivative can be used to detect cysteine (Cys) and homocysteine (Hcy) simultaneously in neutral media. The method involves thioether formation followed by

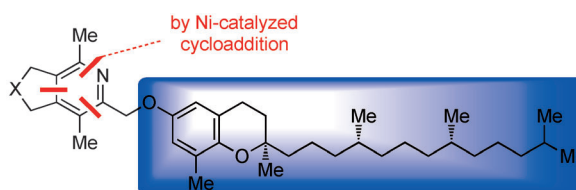
cyclization to release 2-(2'-hydroxy-3'-methoxyphenyl)benzothiazole (HMBT) and a lactam. The differences in ring-formation kinetics allow spectral or kinetic modes to be used to identify Cys and Hcy.

Heterocycles

P. Kumar, S. Prescher,
J. Louie* — 10694 – 10698



A Serendipitous Discovery: Nickel Catalyst for the Cycloaddition of Dienes with Unactivated Nitriles



In the nick of time! The catalytic combination of $[\text{Ni}(\text{cod})_2]$ (cod = 1,5-cyclooctadiene) and the ligand 4,5-bis(diphenylphosphino)-9,9-dimethylxanthene (Xantphos) was used to access pyridines (see

scheme). The reaction proceeds under ambient conditions to provide excellent yields of the products. Comparison of this catalyst with the other state-of-the-art catalysts is also provided.

Enzymes

L. M. Eubanks, G. N. Stowe,
S. De Lamo Marin, A. V. Mayorov,
M. S. Hixon, K. D. Janda* — 10699 – 10702



Identification of α_2 Macroglobulin as a Major Serum Ghrelin Esterase



Fishing for a protein: An analogue of the appetite-stimulating hormone ghrelin containing a phosphonofluoridate moiety and a terminal alkyne functions as a probe to capture the protein α_2 macroglobulin

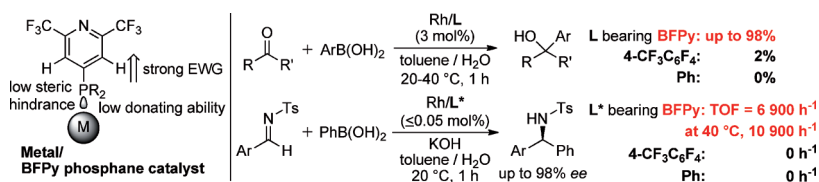
(red; see picture). The extraction of the protein is highly selective and a previously undocumented catalytic activity of α_2 macroglobulin as a hydrolase for ghrelin has been identified.

P Ligands

T. Korenaga,* A. Ko, K. Uotani, Y. Tanaka,
T. Sakai* — 10703 – 10707

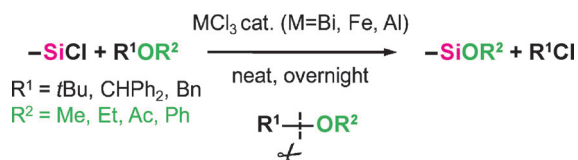


Synthesis and Application of 2,6-Bis(trifluoromethyl)-4-pyridyl Phosphanes: The Most Electron-Poor Aryl Phosphanes with Moderate Bulkiness



The poor will be rich: BFPy phosphanes (see scheme) mimic the electronic and steric characters of $\text{P}(\text{C}_6\text{F}_5)_3$ and PPh_3 , respectively. These novel ligands showed a large ligand acceleration effect on Stille

coupling, the Rh-catalyzed 1,2-addition of aryl boronic acid to unactivated ketones and the asymmetric arylation of *N*-tosylamine using phenylboronic acid.



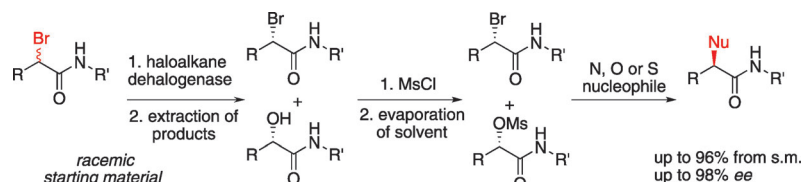
Alcohol-free: A versatile, efficient, and practical synthesis of alkoxy-silanes without generation of HCl involves the reaction of chlorosilanes with unsymmetrical ethers in the presence of a Lewis acid (see

scheme). The reaction proceeds through selective cleavage of C–O bonds and is superior to conventional processes. Industrially feasible reagents are used and only one by-product results.

Synthetic Methods

R. Wakabayashi, Y. Sugiura, T. Shibue,
K. Kuroda* 10708–10711

Practical Conversion of Chlorosilanes into Alkoxy-silanes without Generating HCl



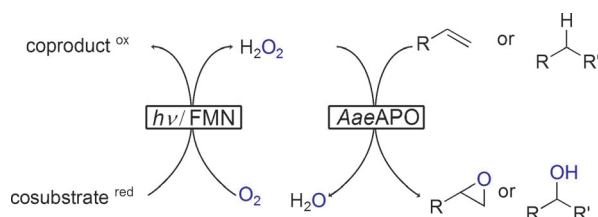
Simple and efficient: The combination of an enzymatic, enantioinverting reaction with simple follow-up processes allows the transformation of readily available racemic compounds into versatile chiral α -substituted amides (see picture; Ms =

methanesulfonyl). These important building blocks are prepared in high overall yield and enantiomeric excess; the elimination of intermediate purification steps results in a time- and cost-efficient process.

Enantioconvergent Processes

W. Szymański, A. Westerbeek,
D. B. Janssen,*
B. L. Feringa* 10712–10715

A Simple Enantioconvergent and Chemoenzymatic Synthesis of Optically Active α -Substituted Amides



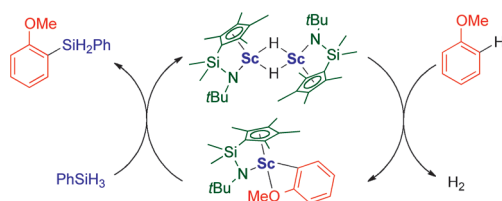
Turn a light on: Enantiospecific hydroxylation of nonactivated C–H bonds as well as epoxidations of C=C bonds are reported using a novel peroxidase from *Agrocyste aegerita* (AaeAPO). AaeAPO represents a more active and more versatile

alternative to the current gold standard, chloroperoxidase. H₂O₂ was produced in situ by photocatalytic reduction of O₂ using simple flavin adenine mononucleotide (FMN) catalysts.

Biocatalysis

E. Churakova, M. Kluge, R. Ullrich,
I. W. C. E. Arends, M. Hofrichter,
F. Hollmann* 10716–10719

Specific Photobiocatalytic Oxygenfunctionalization Reactions



Regioselective, hydrogen-acceptor-free C–H bond silylation of anisoles or alkoxy-substituted benzenes with hydrosilanes was achieved by use of a half-sandwich scandium catalyst. The reaction proceeds

through *ortho*-C–H activation of an anisole compound by a scandium hydride species followed by the silylation of the resulting scandium 2-anisyl species with a hydrosilane (see scheme).

C–H Silylation

J. Oyamada, M. Nishiura,
Z. Hou* 10720–10723

Scandium-Catalyzed Silylation of Aromatic C–H Bonds



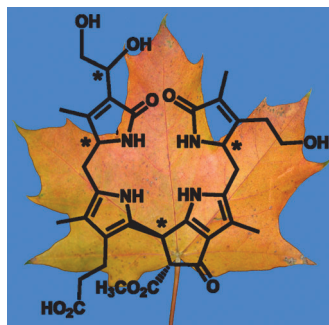
Chlorophyll Catabolites



T. Müller, M. Rafelsberger, C. Vergeiner,
B. Kräutler* _____ 10724–10727



A Dioxobilane as Product of a Divergent
Path of Chlorophyll Breakdown in Norway
Maple



A colorless chlorophyll catabolite was found in senescent leaves of Norway maple, a widespread deciduous tree. This compound is a dioxobilane, a “linear” tetrapyrrole, in which one *meso* carbon of the macrocycle of the hypothetical chlorophyll precursor has been lost. The configuration of this catabolite suggests a path of chlorophyll breakdown in Norway maple that diverges from that found in senescent leaves of other higher plants.

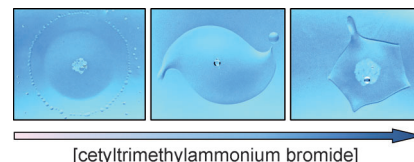
Lifelike Droplets

V. Pimienta,* M. Brost, N. Kovalchuk,
S. Bresch, O. Steinbock* _____ 10728–10731



Complex Shapes and Dynamics of
Dissolving Drops of Dichloromethane

Generation of cohesive motion was observed during the dissolution of mm-sized drops of dichloromethane into aqueous surfactant solutions. This system shows pulsating drops, multi-armed rotors, and polygonal shapes. The sharp tips of these patterns eject much smaller droplets to form expanding halos or swirling chains. The daughter droplets also undergo cascades of secondary and higher-order splitting events.



Supporting information is available
on www.angewandte.org
(see article for access details).



A video clip is available as Supporting
Information on www.angewandte.org
(see article for access details).



This article is available
online free of charge
(Open Access)

Sources

Product and Company Directory

You can start the entry for your company in “Sources” in any issue of *Angewandte Chemie*.

If you would like more information, please do not hesitate to contact us.

Wiley-VCH Verlag – Advertising Department

Tel.: ☎ 62 01 - 60 65 65

Fax: ☎ 62 01 - 60 65 50

E-Mail: MSchulz@wiley-vch.de

Service

Spotlight on Angewandte's
Sister Journals _____ 10484–10486

Preview _____ 10733